World Journal of Applied Physics
2021; 6(4): 60-69
http://www.sciencepublishinggroup.com/j/wjap
doi: 10.11648/j.wjap.20210604.12
ISSN: 2637-5990 (Print); ISSN: 2637-6008 (Online)

Trolleybus Catenary-Pantograph Self-generation Contact Force Under Preload

Min Chen[1, *], Tony Allen[2]

[1]Wolfson School, Loughborough University, Leicestershire, UK

[2]Retired from Nottingham Trent University, Nottingham, UK

Email address:

M.Chen@lboro.ac.uk (Min Chen), mcminchen@gmail.com (Min Chen)

[*]Corresponding author

To cite this article:

Min Chen, Tony Allen. Trolleybus Catenary-Pantograph Self-generation Contact Force Under Preload. *World Journal of Applied Physics*. Vol. 6, No. 4, 2021, pp. 60-69. doi: 10.11648/j.wjap.20210604.12

Received: October 6, 2021; **Accepted**: October 28, 2021; **Published**: November 27, 2021

Abstract: This paper presents part of the research findings from the 'Active Control of Trolleybus Current Collection Systems (ACTCCS)' PhD project undertaken at Loughborough University, UK. In this paper, the issues of preload and self-generation contact force are investigated within a dynamic model and simulation of a 'trolleybus' catenary-pantograph system. The self-generation contact force is created under the preload which they are both interdepend and inseparable each other in any kind of catenary-pantograph system. Under normal operations, the preload and self-generation contact forces help maintain contact between the trolleybus pantograph and catenary overhead power line to prevent arcing, power off or even de-wirement. There are four modellings which are single catenary, initial position of pantograph under preload, Integration of a trolleybus' catenary-pantograph and combination of trolleybus catenary-pantograph system with self-generation contact force to be gradually built as well as the simulations were carried out. The results of simulations show that there is significant different with and without self-generation contact force. Put other words, the trolleybus catenary-pantograph system cannot work properly, even cannot completely work without self-generation contact force. Except trolleybus, the conclusion from modelling and results can also be applicable to all kinds of catenary-pantograph systems including electricized trains, trams, and metros etc.

Keywords: Preload, Self-generation Contact Force, Catenary, Pantograph and Trolleybus

1. Introduction

Electrical transportation systems are seen as one of the key technologies for helping urban public transport methods moderate their impact on global climate change. As such, trams (or re-invented as light rail) have been now coming back to in both the UK [1] and European cities. However, the huge infrastructure cost and time overruns involved in their creation are still a barrier to new tram systems being implemented [1]. One of the main costs associated with the re-introduction of tram systems is the installation of new tram lines either within or next to existing public highways in additional to the overhead power line infrastructure. Consequently, a re-invented trolleybus, that only requires installation of the overhead power-line infrastructure in order to run easily on existing public highways, could be an alternative solution for near future urban public transport. Siemens are currently developing their eHighway project, which has been tested in several countries [2, 3]. Loughborough University in the UK has also been studying a new concept trolleybus with an Active Control of Trolleybus Current Collection System (ACTCCS) as shown in Figure 1.

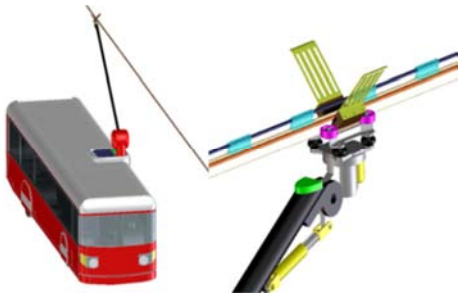

Figure 1. *New concept trolleybus (left) with ACTCCS controlled pantograph-head and single overhead catenary with two wires separated by an insulation strip (right).*

In reality, the catenary-pantograph system of a trolleybus is an interactive system formed by the catenary wire and the pantograph head. As a consequence, this study needed to create and integrate separate models of the catenary wire, pantograph position and self-generation contact force in order to create an integrated dynamic model of a trolleybus catenary-pantograph system.

2. Model of Single Catenary

Basing on a pure trolleybus contact wire (without messenger cable [4]), the vertical displacement of single catenary (called "catenary" hereafter) wire with nominal stiffness for trolleybus' pantographs are shown in Figure 2. Note. In Matlab the independent variable of x is replaced by v·t to transfer the two dimensions-space coordinates into space-time coordinates [5] with matchable rulers between space and time.

The vertical displacement and stiffness of the catenary are defined in $Z_c(t)$ (modified from reference [6]) and $K_c(t)$ [7].

$$Z_c(t) = \frac{g \cdot \rho}{2T_c}\left(v \cdot t - \frac{L_{ws}}{2}\right)^2 - \frac{g \cdot \rho}{8T_c}(L_{ws})^2$$

$$= \frac{g \cdot \rho}{2T_c}[(v \cdot t)^2 - (v \cdot t) \cdot L_{ws}] \quad (1)$$

$$K_c(t) = k_{mean}\left(1 - a\cos\frac{2\pi}{L_{ws}} v \cdot t\right) \quad (2)$$

$$Where: k_{mean} = \frac{k_{max} + k_{min}}{2}, a = \frac{k_{max} - k_{min}}{k_{max} + k_{min}}$$

Note: $Z_c(t)$ keeps zero or negative and $K_c(t)$ keeps positive at any time. To be simply assumed that $Z_c(t)$ stays at the balanced position between gravity ($g \cdot \rho$) and the tension of the catenary. In addition, the length of catenary is also assumed a constant without change in any condition in this model.

3. Initial Position of Pantograph Under Preload

If without downward force from the catenary wire, the pantograph would freely reach its maximum position pushed up by lift force from pantograph spring mounted on the base. As the contribution of the preload lift force from the pantograph-head spring could be ignored, the initial position of the pantograph would then be at the balance point (rising angle) of the gravitational force on the pantograph and the preload lift force provided by the pantograph-boom spring. Note. As the size of pantograph-head is considerably smaller than the pantograph-boom, the size of pantograph-head was not taken into account of position of the pantograph. The pantograph of the trolleybus at its lowest, highest and initial positions are schematically shown in Figure 3. Note. the physical.

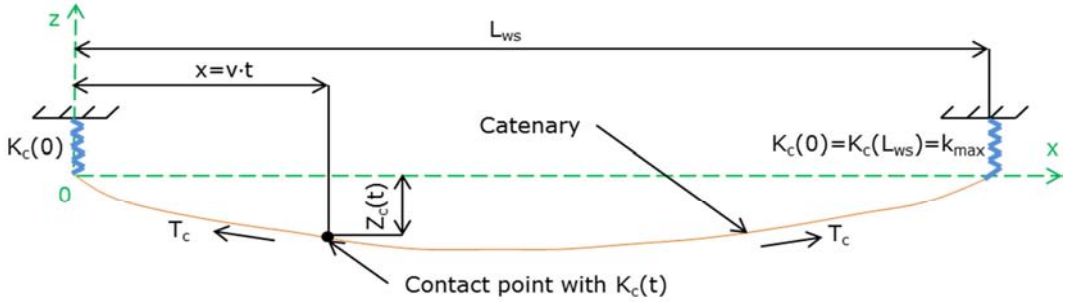

Figure 2. *Trolleybus Catenary (single) model.*

The equations are shown below:

restriction that is positioned to prevent the pantograph from accidently going beyond the highest set position (virtual) should never be reached, so any force from this hard constraint was not included in the model.

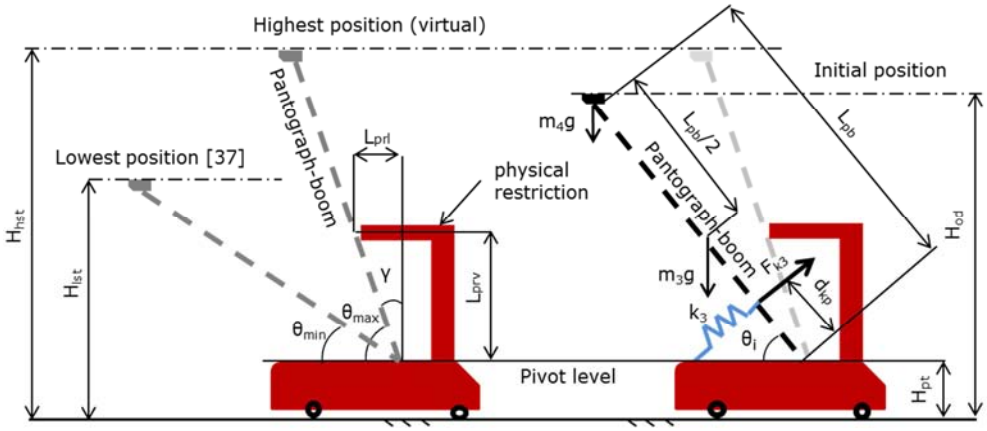

Figure 3. *Schematic diagram of the trolleybus pantograph at its highest virtual and initial positions.*

The actual physical characteristics of a real pantograph on a trolleybus were measured [8] and used to calculate the maximum and initial positions of the pantograph under preload. The pantograph was assumed to be at its highest position when the spring (k_3) was fully relaxed under an adjustment [9]. The equations and derivation are shown in (3), (4) and (5) which are referring to the left-side of Figure 3.

$$\tan\gamma = \frac{L_{prl}}{Lprv} = \frac{0.125}{0.40} \approx 0.286 \quad (3)$$

$$\therefore \gamma \approx 17.4^o; \ \therefore \ \theta_{max} \approx 90^o - 17.4^o = 72.6^o$$

$$H_{hst} = L_{pb} \cdot \cos\gamma + H_{pt} = 6 * \cos 18.4^o + 3.5 \approx 9.2m \quad (4)$$

The pantograph lowest lifting angle θ_{min} is simply given by

$$\theta_{min} = sin^{-1}\frac{H_{lst} - H_{pt}}{L_{pb}} = \frac{4.7-3.5}{6} \approx 11.5^o \quad (5)$$

Referring to right-side of Figure 3, the preload lift force (provide by k_3) and the gravitational force on the pantograph (including boom and head) are in balance at the initial pantograph position. The torque equations corresponding to this position are shown in (6) and (7) as well as their solution in (8).

$$F_{k3} \cdot d_{kp} = m_4 \cdot g \cdot L_{pb} \cos\theta_i + m_3 \cdot g \cdot \frac{L_{pb}}{2} \cos\theta_i \quad (6)$$

$$F_{k3} = k_3 \cdot d_{kp} \cdot tan\,\theta_i \quad (7)$$

$$\therefore sin\,\theta_i = \frac{-3k_3 \cdot d_{kp}{}^2 + \sqrt{\left(3k_3 \cdot d_{kp}{}^2\right)^2 + 16(m_4+m_3)^2 \cdot g^2 \cdot L_{pb}{}^2}}{4(m_4+m_3)g \cdot L_{pb}} \quad (8)$$

4. Integrated Model of the Trolleybus' Catenary-pantograph and Simulation Results

4.1. Modelling

Under equilibrium, the models of the catenary and initial position of pantograph have been determined according to Figure 3. In operation, the modelling could be assumed that the trolleybus pantograph swinging around a lifting angle θ by a constrained angular movement Δθ, as shown in Figure 4.

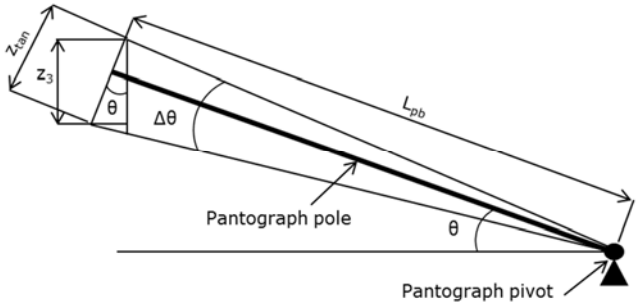

Figure 4. *Movement of trolleybus pantograph around a lifting angle θ with a constrained angular movement Δθ.*

Integrating all these models and assumptions, a full model of a trolleybus catenary-pantograph system was built as shown in Figure 5.

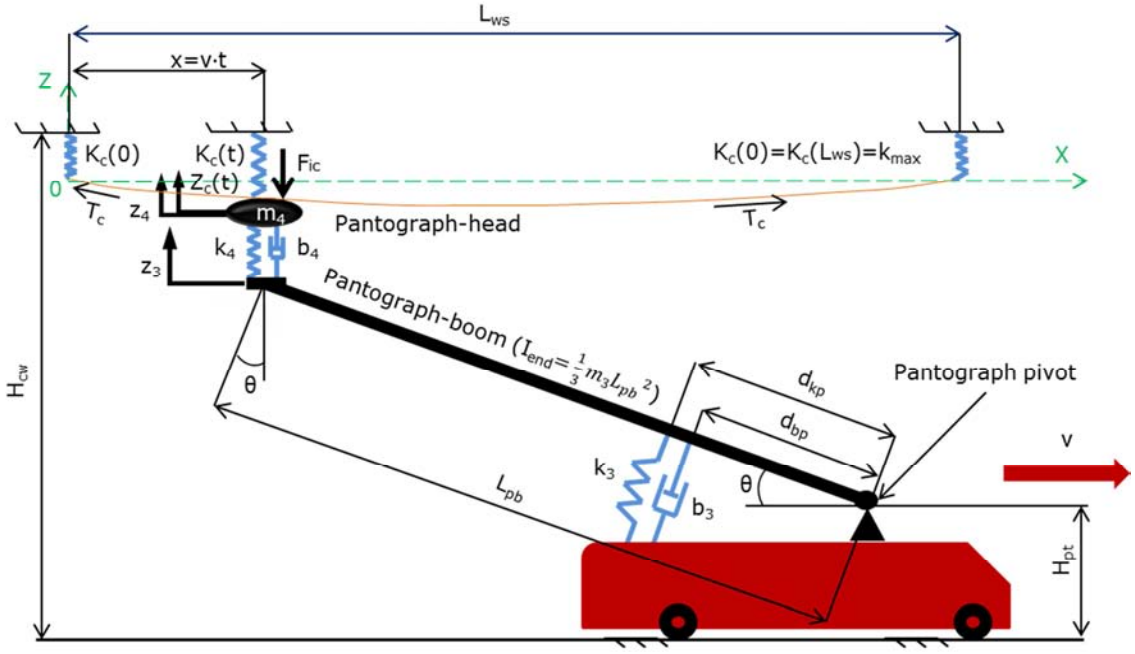

Figure 5. *Catenary-pantograph model of trolleybus.*

Note: As the trolleybus is an urban transport system with an operational speed which is lower 70% than catenary wave propagation speed [10], therefore the catenary wave propagation speed was not taken into account into the modelling of the catenary-pantograph system in this paper. In addition, any effects of the trolleybus suspension system were not a consideration of this paper.

By Newton's second law of linear and rotary motion, a dynamic model of the catenary-pantograph system, shown in Figure 4. and Figure 5, was derived as follows:

$$I_{end} \cdot \Delta\ddot{\theta} = -b_3 \cdot \dot{z}_3 \cdot \frac{d_{bp}}{L_{pb}} \cdot cos\,\theta \cdot d_{bp} - k_3 \cdot z_3 \cdot \frac{d_{kp}}{L_{pb}} \cdot \cos\theta \cdot d_{kp} + b_4 \cdot (\dot{z}_4 - \dot{z}_3) \cdot cos\,\theta \cdot L_{pb} + k_4 \cdot (z_4 - z_3) \cdot cos\,\theta \cdot L_{pb} \quad (9)$$

$$m_4 \ddot{z}_4 = -b_4(\dot{z}_4 - \dot{z}_3) - k_4(z_4 - z_3) - F_{ic} \quad (10)$$

$$where:\ I_{end} = \frac{1}{3} \cdot m_3 \cdot {L_{pb}}^2$$

In (10), the interactive contact force between the catenary and pantograph-head (F_{ic}) can be thought of as a dynamic contact force.

As the dynamic displacement of the pantograph is not great than 70mm [12, 13], thus the dynamic angular movement with 6.0m length pantograph-boom (L_{pb}) is smaller than ($\Delta\theta \leq 15^o$). The following approximation could therefore be made that is smaller than 1% in the sine and 2% in the tangent values from the true measurement of the angle [14].

$$\Delta\theta = \frac{Z_{tan}}{L_{pb}} = \frac{z_3}{L_{pb} \cdot cos\,\theta};\ where\ z_3 = Z_{tan} \cdot \cos\theta \quad (11)$$

$$\Delta\ddot{\theta} = \frac{\ddot{z}_{tan}}{L_{pb}} = \frac{\ddot{z}_3}{L_{pb}\cos\theta} \quad (12)$$

In addition, simplified equations (9) can be re-written or re-ordered as (13):

$$m_3 \ddot{z}_3 = -b_{3eq} \cdot \dot{z}_3 \cdot cos^2\theta - k_{3eq} \cdot z_3 \cdot cos^2\theta + 3b_4(\dot{z}_4 - \dot{z}_3) \cdot cos^2\theta + 3k_4(z_4 - z_3) \cdot cos^2\theta \quad (13)$$

$$where: b_{3eq} = 3b_3 \cdot \frac{{d_{bp}}^2}{{L_{pb}}^2};\ k_{3eq} = 3k_3 \cdot \frac{{d_{kp}}^2}{{L_{pb}}^2}$$

The integrated contact force between the catenary wire and pantograph-head (F_{ic}) is dynamically, this contact force could be thought only generated during the trolleybus in operation. This dynamic force is of course related to the displacement ($Z_c(t)$) and stiffness $K_c(t)$ of the catenary wire as well as the pantograph-head vertical displacement (z_4). The final equation is shown in (14).

$$F_{ic} = K_c(t) \cdot [z_4 - Z_c(t)] \quad (14)$$

4.2. Simulation Results and Analysis

By using Simulink to carry out the simulation, the various conditions and parameters have been determined from real-world trolleybus operations. For simplicity, two typical operating speeds were considered in this simulation as shown in

Table 1. *Selected trolleybus velocities for simulation.*

Condition	In depot	On street
Speed V(m/s)	1.0	14.0

Table 1. The "In depot" models consider the very low velocity used within in a tram depot. The "On street" models consider the regulation speed 30 mph (13.3m/s) used in British towns [15].

To estimate the useful parameters, the measurements of an old-style trolleybus, as given by Mr Tim Stubbs [16], was carried out and applied to the modelling and simulations.

The measured mass of the pantograph combination used is 76.6kg (single pole and hub) [16]. With considering of additional masses of actuators and relevant mechanism (approximate 20kg), power cables (approximate 17kg, 95mm^2, 600-1000V.) and bolts (approximate 10kg) etc. [17, 18], the total mass of pantograph m_3 would be 120 kg.

$$m_3 \approx 120(kg)$$

Some of the other required specifications of a trolleybus pantograph and the catenary wire could not be obtained from refence materiel. Consequently, all other required data for the simulation had to be gathered from practice measurement at the Trolleybus Museum at Sandtoft [19] and Crich Tramway Village [20] as well as references in light rail (modified referring to the [21, 22]) area. The complete specifications used are as shown in Table 2.

Table 2. *Selected parameters for simulation of a trolleybus' catenary-pantograph system.*

Parameters	m_3 (kg)	k_3 (N/m)	b_3 (Ns/m)	m_4 (kg)	k_4 (N/m)	b_4 (Ns/m)	
Value	120	24000 [8]	150	4	7000	30	
Parameters	L_{pb} (m)	d_{kp} (m)	d_{bp} (m)	θ_{max} (degree)		v (m/s)	g (m/s^2)
Value	6.0	0.1	0.1	72.3		1, 14	9.18
Parameters	L_{ws} (m)	T_c (N)	H_{cw} (m)	H_{pt} (m)	ρ (kg/m)	k_{min} (N/m)	k_{max} (N/m)
Value	30	10^4	5.5	3.5	0.95 [22, 23]	1000	3000

After applying these parameters into the catenary & pantograph models, the simulated values of catenary & pantograph-head vertical displacement ($Z_c(t)$ & z_4) and interactive contact force (F_{ic}) between the catenary and pantograph-head, shown in Figure 6 and Figure 7, were obtained:

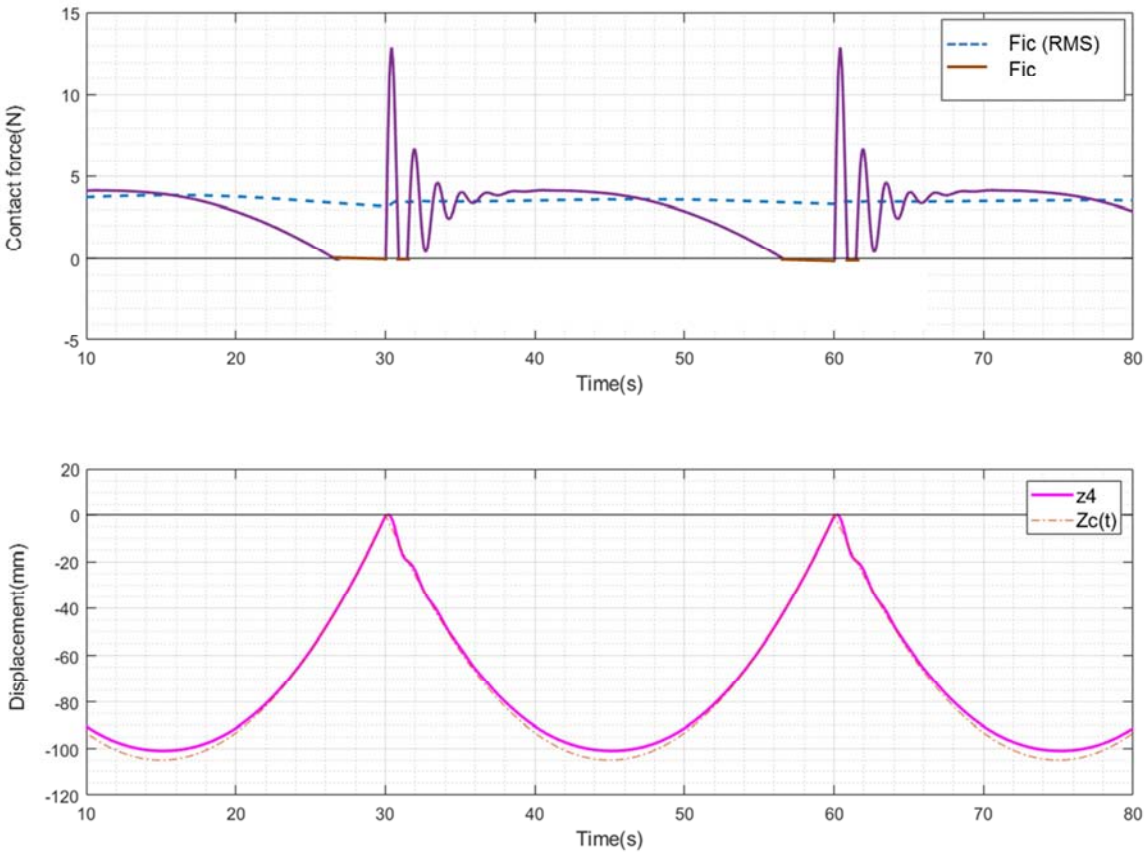

Figure 6. *Simulation result of trolleybus' catenary-pantograph at v=1m/s (In depot speed).*

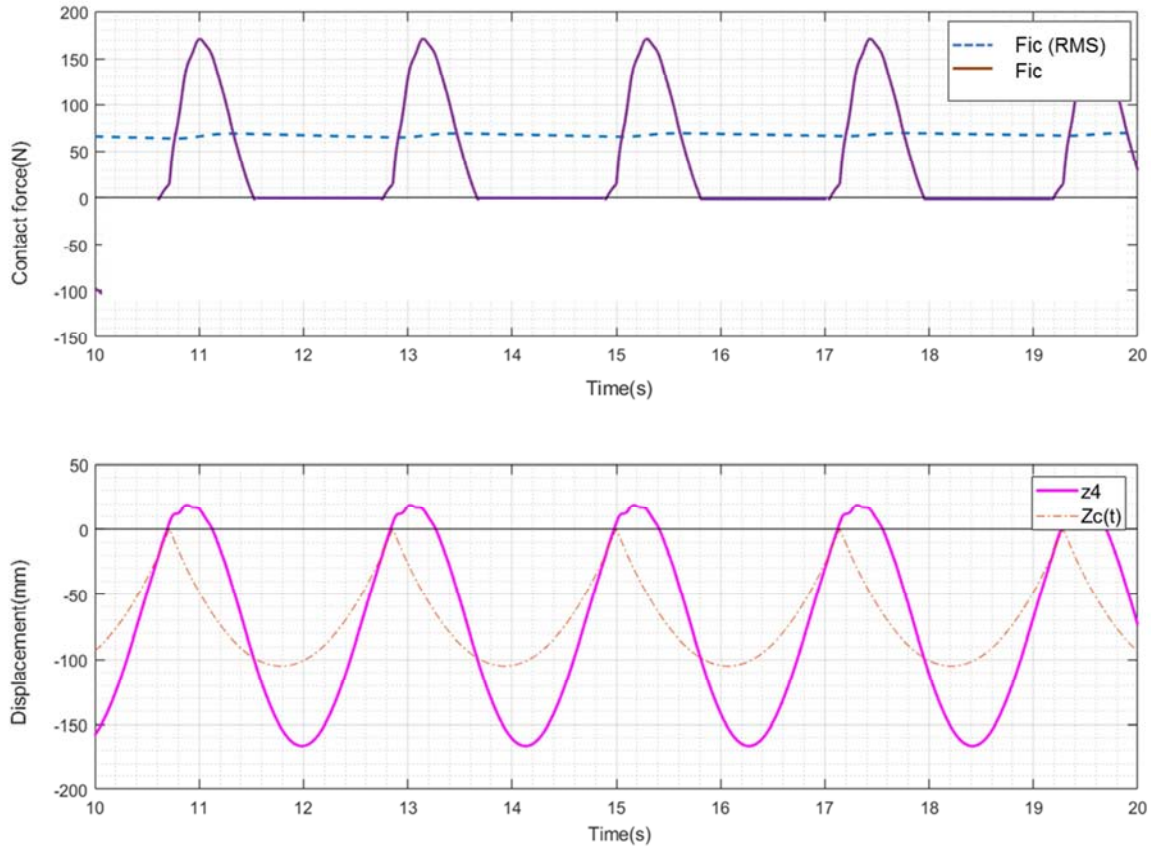

Figure 7. *Simulation result of trolleybus' catenary-pantograph at v=14m/s (On street speed).*

From Figure 6, at v=1m/s (In depot speed) the simulated value of interactive contact force (F_{ic}) varies between 0 and 13N with an average value around 4N. This is much lower than the requirement standard (80 to 130N) [7] and significantly lower than the static contact force practically measured (33 to 145N) in museums and modern tram deport [19, 20, 24]. In addition, the simulation value of the contact between the catenary and pantograph is essentially unstable with periodic contact loss (F_{ic}=0).

From Figure 7, it can be seen that at v=14m/s speed (On street speed) there is a higher variation in the simulated value of interactive contact force (F_{ic}) with longer periods of contact loss (Fic=0).

In addition, it can be seen in Figures 6 and Figure 7 that the displacement of the pantograph-head at both speeds is periodically lower than catenary wire displacement. This means that the pantograph-head is repeatedly without stable electric supply and at serious risk of de-wirement. Under such operating conditions, it is clear that, any Trolleybus' catenary-pantograph system that operated as per the models developed in this section using the existing Trolleybus theory & measurements would not work.

Overall, it is obvious that the initial simulation results do not make sense and cannot be a realistic model of a real trolleybus system. Therefore, a further study was carried to resolve the issue as explained in the next chapter.

5. Integrated Model with Self-generation Contact Force and Simulation Results

5.1. Modelling

As stated in the last section, the initial simulation models of the trolleybus catenary-pantograph did not satisfy either the theoretical or practical expectations of a real trolleybus system. Therefore, a new kind of contact force called the self-generation contact force (F_{sg}) was postulated for the trolleybus' catenary-pantograph system as well as being created under the preload which they are both interdepend and inseparable each other.

The self-generation contact force (F_{sg}) between the catenary wire and pantograph-head is defined to be generated by the compressed pantograph-head (with stiffness k_4) and pantograph-boom (with stiffness k_3). This kind contact force is due to the pantograph-head with pantograph-boom being forcedly pushed down by the catenary wire which installation level is much lower than the initial position of pantograph-head. The contact force remains as long as the pantograph is engaged with the catenary wire. As a special example that the self-generation contact force is equal preload with opposite direction when trolleybus is static at v=0m/s. This applies to all kinds of electrified transport system such as trolleybus, light railways and trains and is the essential contact force that reduces variation in the dynamic contact force.

F_{sg} is a complex dynamic force that depends on the displacement ($Z_c(t)$) and stiffness $K_c(t)$ of the catenary wire as shown in Figure 8. This self-generation force can be thought of as the pantograph lifting force acting on the catenary wire as it moves up or down with different displacements. Among all the possible displacements that the deflection of the catenary may follow, called virtual displacements [25], the self-generation force can be assumed and treated as a non-conservative force [26] as shown in equation (15).

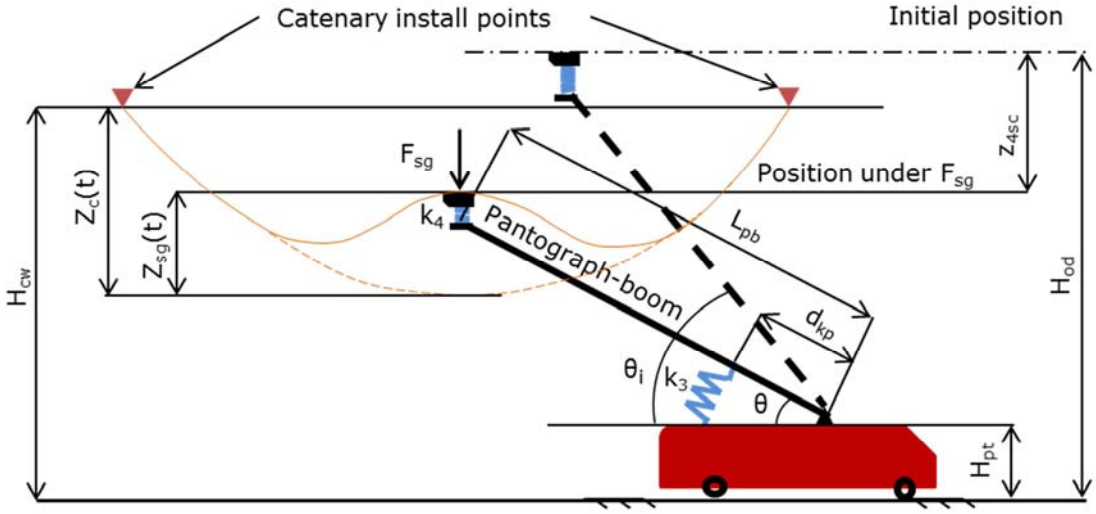

Figure 8. *Model of self-generation force (F_{sg}).*

Following Hooke's law and geometrics, the equations of the self-generation force (F_{sg}) were deduced as shown below:

$$F_{sg} = \frac{k_{3eq} \cdot k_4}{k_{3eq} + k_4} \cdot z_{4sc} = Kc(t) \cdot Z_{sg}(t) \quad (15)$$

$$H_{od} = z_{4sc} + Z_{sg}(t) + H_{cw} - Z_c(t) \quad (16)$$

Using both (E5.1) and (E5.2), z_{4sc} can be deduced as (17)

$$z_{4sc} = \frac{H_{od} - H_{cw} + Z_c(t)}{1 + \frac{k_{3eq} \cdot k_4}{K_c(t) \cdot (k_{3eq} + k_4)}} \quad (18)$$

A further derivation can be made to get (19) for F_{sg}

$$F_{sg} = \frac{k_{3eq} \cdot k_4}{k_{3eq} + k_4} \cdot \frac{H_{od} - H_{cw} + Z_c(t)}{1 + \frac{k_{3eq} \cdot k_4}{K_c(t) \cdot (k_{3eq} + k_4)}} \quad (19)$$

Therefore, the total interactive contact force (F_{totic}) between the catenary wire and the pantograph-head should be the sum of this self-generation force and the original interactive contact force derived in section 4 (F_{ic}). This is shown in (20)

$$F_{totic} = F_{sg} + F_{ic}$$

$$F_{totic} = \frac{k_{3eq} \cdot k_4}{k_{3eq} + k_4} \cdot \frac{H_{od} - H_{cw} + Z_c(t)}{1 + \frac{k_{3eq} \cdot k_4}{K_c(t) \cdot (k_{3eq} + k_4)}} + K_c(t) \cdot [z_4 - Z_c(t)] \quad (20)$$

As the gravitational force on the catenary wire ($g \cdot \rho$) is an element of the pre-vertical displacement of the preloaded catenary wire $Z_c(t)$ (defined by (1)), the total interactive contact force includes a contribution from catenary wire gravity.

From Figure 8, the equation of sinθ can be deduced as shown in (21) with (18)

$$sin\,\theta = \frac{H_{od} - H_{pt} - z_{4sc}}{L_{pb}} \quad (21)$$

Integrating all these derivations, the final model of the integrated trolleybus catenary-pantograph system is as shown in (10), (13), (20) and (21).

5.2. Simulation Results and Analysis

The second simulation was carried out using Simulink with the conditions and parameters determined in section 4.

After applying these parameters into the simulation models the values of catenary & pantograph-head vertical displacement ($Z_c(t)$ & z_4) displacement and total interactive contact force (F_{totic}) between the catenary and pantograph-head, shown in Figures 9 and Figure 10, were obtained:

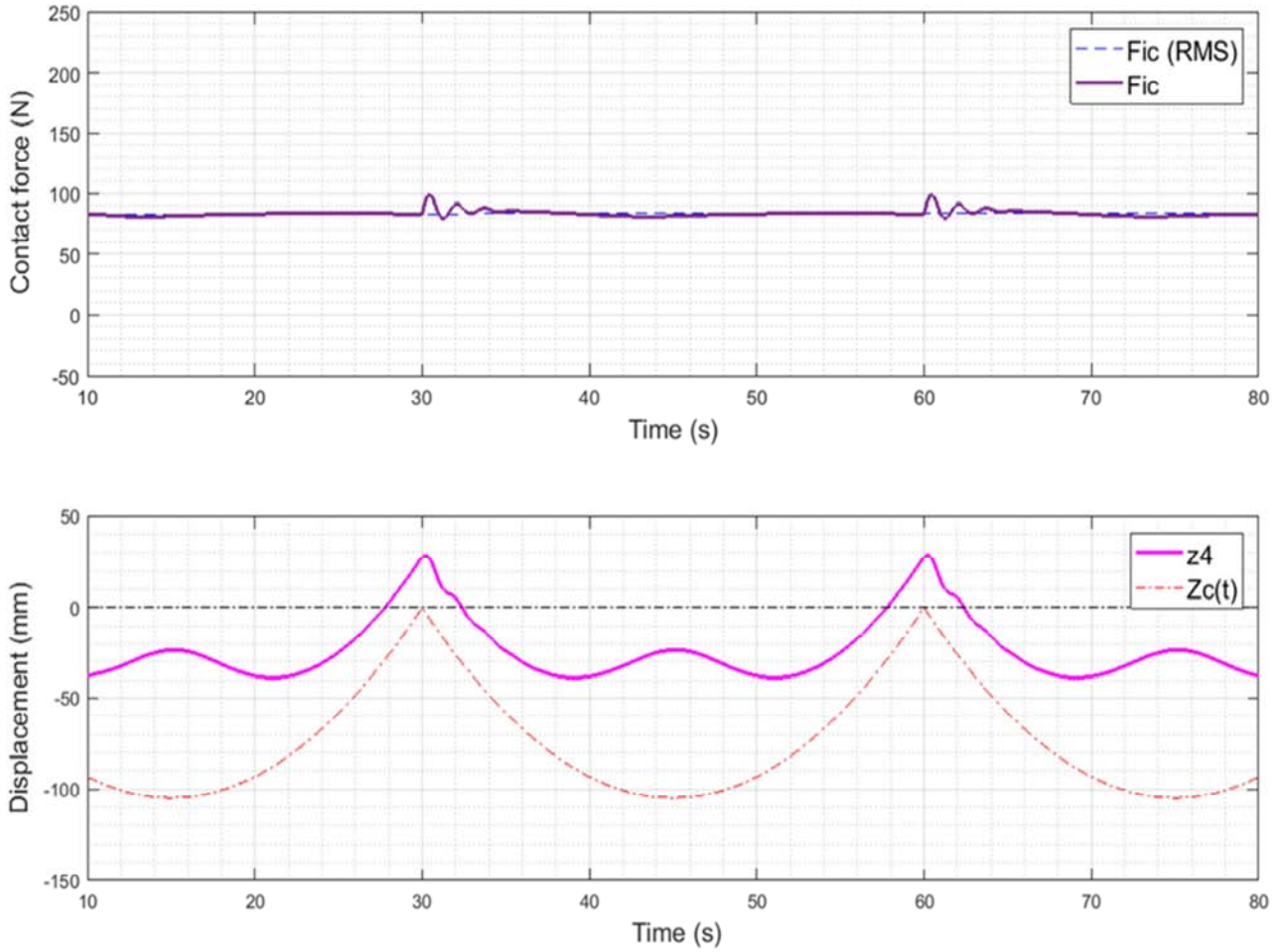

Figure 9. *Simulation result of trolleybus' catenary-pantograph with self-generation contact force at v=1m/s (In depot speed).*

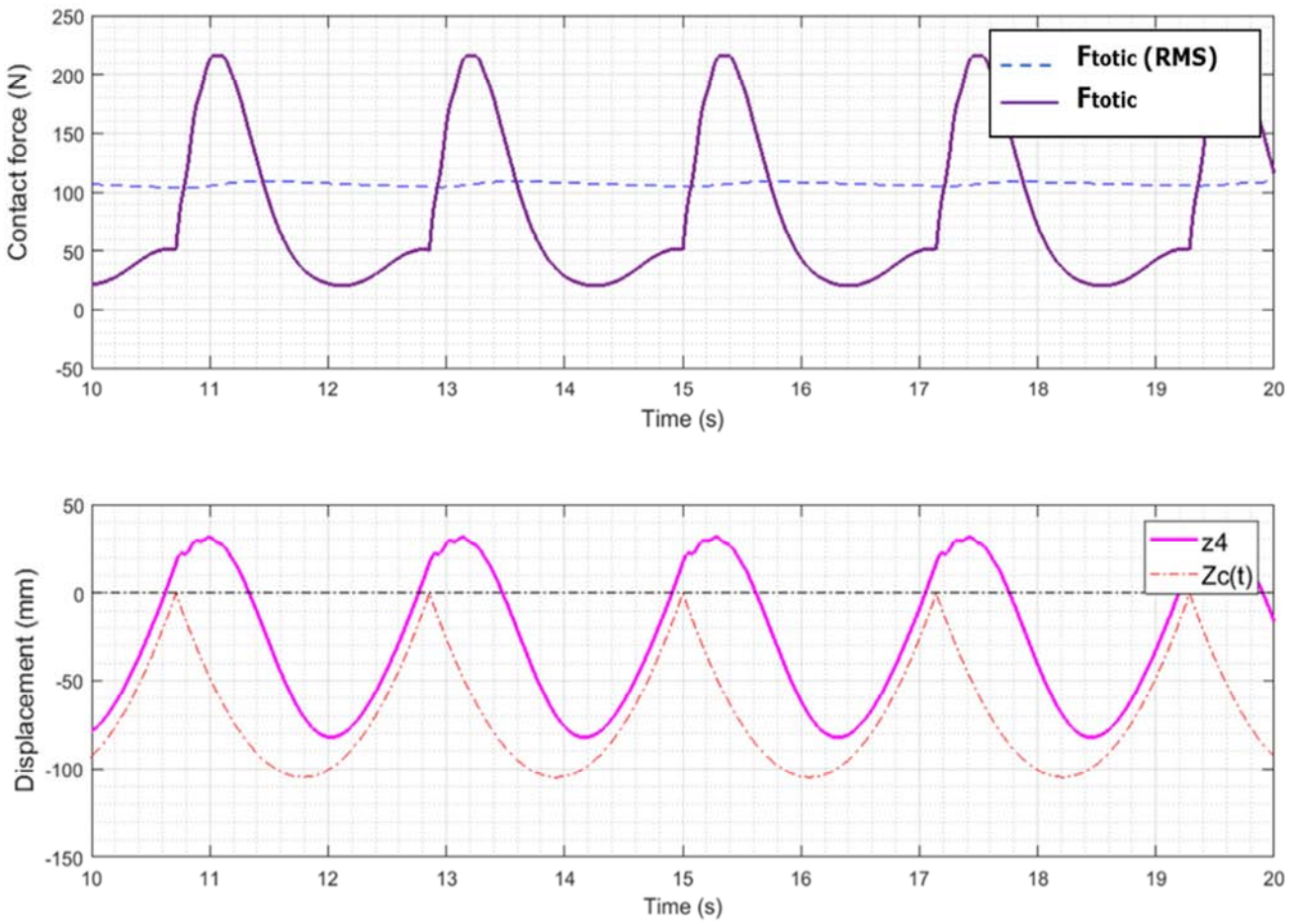

Figure 10. *Simulation result OF Trolleybus' catenary-pantograph with self-generation contact force at v=14m/s (On street speed).*

From Figure 9, it can be seen that at v=1m/s speed (In depot) the interactive contact force (F_{totic}) value of 84N is close to the average real value of the static contact force of 89N (v=0) measured at the trolleybus museum and the tram depot in Sheffield [19, 24].

From Figure 10, it can be seen that at v=14m/s speed (On street) the higher interactive contact force (F_{totic}) and lower contact force deviation with no contact loss (F_{totic} = 0) is a more reasonable model of a working Trolleybus' catenary-pantograph system than the original integrated model developed in section4.

In finally, Figures 9 and Figure 10 show that the displacement of the pantograph-head at both speeds is always higher than the catenary displacement; indicating that the pantograph-head maintains a continuous electric supply and has little possibility of de-wirement.

6. Conclusion

A statistical analysis of the interactive contact force simulations shown in Figures 6 and Figure 7, Figures 9 and Figure 10 were performed using Time Scope in the DSP system of Simulink. The results obtained are listed in Table 3.

Table 3. *Statistical analysis of the F_{ic} and F_{totic} simulation results and comparison between with and without self-generation contact force.*

Interactive contact force (Total) (N) Speed (m/s)	$F_{totic/ic}$ (RMS)	$F_{totic/ic}$ (Max)	$F_{ic/totic}$ (Min)	Variation (Max-Min)
1.0 (with self-generation contact force)	80	100	79	21
1.0 (without self-generation contact force)	4	13	0	13
14.0 (with self-generation contact force)	105	216	20	196
14.0 (without self-generation contact force)	65	170	0	170

1) $F_{totic/ic}$ (RMS): The effective value of contact force in positive defines the quality of general contact performance between the pantograph-head and catenary wire.
2) $F_{totic/ic}$ (Max) and (Min): As the transient contact force (both in positive and zero) between the pantograph-head and catenary wire, which could be in use to estimate the possible risk of de-wirement or electric arcing.
3) The Variation of $F_{totic/ic}$: To evaluate wearing disequilibrium in different section along the catenary wire between the poles.

It is clear from Table 3 that for a trolleybus running at

speeds of 1.0m/s (In depot) and 14m/s (On street) the integrated contact force with self-generation contact force (F_{totic}) has a significantly increased RMS, Max & Min values compared to the original integrated contact force (F_{ic}). There is some increase in the Variation of F_{totic} when the self-generation contact force is included in the interactive contact force. However, this increase in variation does not affect the running of the system as it does not include any contact loss (F_{totic} = 0) periods. The additional contribution from the self-generation force (F_{sg}) effectively ensures that periodic contact loss is prevented. Consequently, a stable electric supply is continuously provided and there is little risk of de-wirement. The final integrated models developed in section 5 are thus a reasonable model of a real-world Trolleybus' catenary-pantograph system

Finally, it is expected that the dynamic self-generation contact force under preload simulated here are a natural characteristic of all kinds of catenary-pantograph systems and play a significant role in keeping all catenary-pantograph systems stable.

Nomenclature [27]

b_3: damping rate of pantograph-boom (Ns/m)

b_4: damping rate of pantograph-head (Ns/m)

d_{bp}: distance between damper fitting point and pantograph pivot point (m)

d_{kp}: distance between spring fitting point and pantograph pivot point

F_{ic}: interactive contact force between catenary and pantograph-head (N) [9]

F_{ic} (RMS): interactive contact force (RMS) between catenary and pantograph-head (N)

F_{k3}: lift force provided by k_3 as preload (N)

F_{sg}: self-generation contact force (N)

F_{totic}: total interactive contact force between catenary and pantograph-head (N)

F_{totic} (RMS): total interactive contact force (RMS) between catenary and pantograph-head (N)

g: gravitation acceleration (9.8m/s^2)

H_{cw}: height of the catenary wire fixed point from ground [7]

H_{hst}: highest position of pantograph-head from ground (m)

H_{lst}: lowest applicable position of pantograph-head from ground (4.7 m) [7]

H_{od}: initial position of pantograph-head from ground (m)

H_{pt}: pivot height of pantograph from ground (3.50 m)

I_{end}: pantograph-boom moment of inertia (kg·m^2)

k_3: nominal stiffness of pantograph-boom spring (N/m)

k_4: stiffness of pantograph-head spring (N/m)

$K_c(0) = K_c(L_{ws})$: catenary stiffness at both poles fix points (N/m) = k_{max}

$K_c(t)$: nominal stiffness of catenary at contact point (N/m)

k_{max}: maximum stiffness of catenary (N/m)

k_{mean}: average stiffness of catenary (N/m)

k_{min}: minimum stiffness of catenary (N/m)

L_{pb}: pantograph-boom length (6.0 m)

L_{prl}: effective level limitation of physical restriction (0.125 m)

L_{prv}: effective vertical limitation of physical restriction (0.40 m)

L_{ws}: catenary span between two poles (m)

m_3: pantograph-boom mass

m_4: pantograph-head mass (kg)

T_c: tension of catenary (N)

v: trolleybus speed (m/s)

x: contact point distance from 0 of x-axis (x=v·t) (m)

z_3: pantograph-boom higher-end vertical displacement (m)

z_4: pantograph-head vertical displacement (trajectory) (m)

z_{4sc}: distance between initial position of pantograph-head from ground (H_{od}) and balance position of pantograph-head under self-generation force (m).

$Z_c(t)$: original vertical displacement of catenary

$Z_{sg}(t)$: vertical displacement of catenary under the self-generation force (m)

Z_{tan}: pantograph boom higher-end tangent displacement (m)

α: Stiffness variation coefficient

γ: pantograph-boom (with head) angle between pantograph and vertical line (degrees) at highest position

ρ: catenary linear mass per unit length (kg/m)

θ: pantograph-boom (with head) dynamic lifting angle (degrees)

Δθ: constrained angular movement

θ_i: pantograph-boom (with head) initial lifting angle (degrees) under preload

θ_{max}: pantograph-boom (with head) highest lifting angle (degrees)

θ_{min}: pantograph-boom (with head) preferred lowest lifting angle (degrees)

Acknowledgements

As one of authors, Min Chen, I would be grateful to Dr Christopher Ward, Dr Ella-Mae Hubbard and Dr Peter Hubbard who, as the supervisors in Loughborough University, UK contributed to professional supervision and supports to my PhD study of ACTCCS (Active Control Trolleybus Current Collection System) which is base of this paper.

References

[1] Sellick, Rebeka, Market Research Summary Report, Innovations, Engineering and Business Consultancy, 2016, [Cited 2016 September]. Available from: rsellick@trl.co.uk, Sat 24/09/2016 07:06.

[2] Manfred Boltze, eHighway–An Infrastructure for Sustainable Road Freight Transport, CIGOS 2019, Innovation for Sustainable Infrastructure pp 35-44.

[3] Rob Clymo, Siemens eHighway promises sustainable road freight transport, our future mobility might be all-electric and data-driven, December 24, 2019. Available from: https://www.techradar.com

[4] Ken Shores; Catenary on Japanese Railroads; Sumida Crossing, An N-Scale, Japanese-Themed, Urban Railroad 2014. Available from: http://sumidacrossing.org/Prototype/PrototypeCatenary

[5] Edwin F. Taylor and John Archibald Wheeler, Spacetime Physics: Introduction to Special Relativity, Second Edition, 1992.

[6] Gator Trax; Suspension Bridges Module; College of Engineering, University of Florida 2004.

[7] Shahin Hedayati Kia, Fabio Bartolini, Augustin Mpanda-Mabwe, Roger Ceschi; Pantograph-Catenary Interaction Model Comparison; IECON 2010 - 36th Annual Conference on IEEE Industrial Electronics Society.

[8] Mr Tim Stubbs' garage, 1 Highfield Drive, Burton upon Trent. The pantograph measured was from the trolleybus having last been used in service in 1950 in the UK.

[9] BSI British Standards; Railway applications—Rolling stock—Electric equipment in trolleybuses—Safety requirements and connection systems; DD CLC/TS 50502:2008.

[10] 5.24 Wave propagation velocity, BSI Standards; Railway applications — Fixed installations — Electric traction overhead contact lines; EN 50119:2009+A1:2013.

[11] Sung Pil Jung, Young Guk Kim, Jin Sung Paik and Tae Won Park, Estimation of Dynamic Contact Force Between a Pantograph and Catenary Using the Finite Element Method, Journal of Computational and Nonlinear Dynamics October 2012, Vol. 7 / 041006-1.

[12] BS EN 50318. Railway applications. Current collection systems. Validation of simulation of the dynamic interaction between pantograph and overhead contact line, 2002.

[13] Mohammad Mirzapour, T. X. Mei, Detection and isolation of actuator failure for actively controlled railway wheelsets, 2014 UKACC International Conference on Control (CONTROL), July 2014.

[14] Charles H. Holbrow, 2.4 Angles and angular measure, Modern Introductory Physics, Second edition, 2010, p32.

[15] Bus speeds reports, Buses performance data, 2017/2018, Available from: http://content.tfl.gov.uk

[16] Mr Tim Stubbs' garage, 1 Highfield Drive, Burton upon Trent. The pantograph measured was from the trolleybus having last been used in service in 1950 in the UK, Available from: tim.stubbs@highfieldengineering.co.uk, 21/11/2017 5:23pm, 12/09/2018 2:17pm and 14/09/2018 11:50.

[17] SA 3 (BS3), SA Series Servoactuators, Linear Servoactuators, Linearmech S.r.l.Via Caduti di Sabbiuno, 3 - 40011 Anzola dell'Emilia (Bologna), ITALY.

[18] Single Core XLPE/PVC/AWA/PVC Power Cable. Available from: http://objects.eanixter.com

[19] The Trolleybus Museum at Sandtoft. Available from: http://www.sandtoft.org.uk

[20] Crich Tramway Village. Available from: http://www.tramway.co.uk

[21] Yu-Chen Lin, Chun-Liang Lin and Chih-Chieh Yang; Robust Active Vibration Control for Rail Vehicle Pantograph; IEEE Transactions on Vehicular Technology, Vol. 56, No. 4, July 2007.

[22] Product catalogue–Overhead contact lines, Kummler+Matter Ltd; 2012, p 12073-12304/6487.

[23] Eland Cables, Cables & Accessories Rail Cable-Overhead Line | 107mm^2 Contact Wire with ID Groove (Hard Drawn Copper), Eland Product Group: 91. Available from: elandcables.com

[24] Chris Jackson, Stagecoach Supertram Maintenance Ltd, Nunnery Depot, Woodbourn Road, SHEFFIELD, S9 3LS. The pantograph measured was from LR33D made by Brecknell Willis.

[25] Jeffrey Erochko, 5.6 The Virtual Work Method, Introduction to Structural Analysis, Carleton University (Ottawa, Canada). Available from: www.learnaboutstructures.com.

[26] Martin Houde, Chapter 4. Lagrangian Dynamics, Classical Mechanics I, Courses Physics 350/Applied Math 353, University of Western Ontario Canada, Page 80-84.

[27] Min Chen, Christopher. P. Ward, Ella-Mae Hubbard, Peter Hubbard, Modelling and Active Control Designing of Trolleybus Catenary-Pantograph System, 7th IFAC Symposium on Mechatronic Systems MECHATRONICS 2016: Loughborough University, Leicestershire, UK, September 2016.